Decoration of Graphene Oxide with Cobalt(II) Coordinated Silica and its Catalytic Activity for the Synthesis of Functionalized Indenopyrazolones

Mahnaz Mirheidari
University of Kashan Faculty of Chemistry
Javad Safaei-Ghom (safaei@kashanu.ac.ir)
University of Kashan Faculty of Chemistry https://orcid.org/0000-0002-9837-4478

Research article

Keywords: graphene oxide, silica nanoparticles, functionalized graphene oxide, Cobalt(II) chloride, indenopyrazolones derivatives

Posted Date: December 16th, 2020

DOI: https://doi.org/10.21203/rs.3.rs-127252/v1

Abstract

We synthesized functionalized f-SiO_2@GO@Co catalyst through decorating graphene oxide surface using SiO_2 sphere with the help of ethylenediamine ligand and chelation with $CoCl_2.6H_2O$ for increasing the catalyst activity to produce heterogenous catalyst. The heterogenous catalyst was characterized by FT-IR, XRD, SEM, Raman spectra, and TGA. We assessed activity of the catalyst in the synthesis of indenopyrazolones and results demonstrated high activity for the catalyst. The ability of the catalyst to increase the yield and reduction in reaction time as well as high catalytic activity, and recycling are prominent advantages of the catalyst.

Introduction

In last few years, applying carbon-based materials as a catalyst have received considerable attention[1]. Graphene is one forms of carbon as a single layer that its crystalline structure is two-dimensional. Graphene was first discovered in 2004 by Geim and Novoselov [2]. Graphene oxide is an oxidized form of graphene with a two-dimensional (2D) honeycomb structure. A monolayer graphene oxide which is a layer of graphite has various oxygen-containing groups like hydroxyl groups, epoxides, and carboxyl group via oxidation of graphite crystals. The presence of oxygen functional groups on the surface of graphene oxide increase chemical interactions so, graphene oxide can be participated as a desirable support or catalyst in chemical reactions[3–5].

Functionalization of graphene oxide is more beneficial for biomedical, electrochemical, and chemical applications[1]. It can be processed using functionalization of oxygen-containing groups on the basal plane of graphene oxide with different electroactive species[6, 7].Different methods have been developed for the synthesis of graphene oxide but the common method is Hummer with oxidation of graphite using $KMnO_4$ under acidic conditions[8]. The fillers like SiO_2 are often used as corrosion resistant coatings. Then, the proper dispersion of SiO_2 in graphene oxide/epoxy coating can improve corrosion resistance[9, 10]. Also, for improving activity and stability of the catalysts metal-based catalysts are used. Due to the high cost of noble metals, the cheaper metals replace for this purpose such as Fe, Ni, and Co [11].

Nitrogen heterocyclic compounds have attracted a researcher’s interest because they have more applications in biological and other sciences[12]. Pyrazoles are a famous series of five-membered nitrogen heterocycles containing two adjacent nitrogen atoms [13]. Compounds containing pyrazole ring and its derivatives often exhibit different physiological and pharmacological properties such as anticonvulsant[14], antioxidant[15], anticancer[16], and fungicides[17]. Moreover, some compounds with pyrazole ring are used as ligands in transition-metal-catalyzed cross-coupling reactions[18, 19].

Since, indeno[1,2-c]pyrazolones are an important class in synthetic and pharmaceutical chemistry, attempted to implement new eco-friendly strategies for the synthesis of indeno[1,2-c]pyrazolones [20, 21].

In the current literature, we focus on preparation, characterization and application of an efficient heterogenous catalyst based on cobalt(II) coordination on f-SiO_2 functionalized graphene oxide(f-SiO_2@GO@Co) (Scheme1) for the synthesis of cis-3-aryl-3a,8b-dihydro-3a,8b-dihydroxy-1-phenyl-indeno[1,2-c]pyrazol-4(1H)-ones in ethanol at 60^oC.

Experimental

General

All commercially organic compounds were purchased from Sigma-Aldrich and Merck. Melting points of products were recorded by Electrothermal 9200. FT-IR measurements were performed on a Nicolet Magna-IR 550 spectrometer using KBr plates. The NMR spectra were recorded in DMSO-d6 on a Bruker Avance-400 MHz spectrometer. The XRD patterns were obtained by an X' Pert PRO (PHILIPS, PW 1510, Netherland) instrument with Cu-kα radiation (λ = 0.154056 nm). FE-SEM and EDS analysis (MIRA3-TESCAN FESEM) have been used to provide morphological and elements information. The TGA- DTA analysis were performed on a Bahr STA- 503 instrument. Raman spectra were obtained on a Takram N1-541 Raman spectrometer (Teksan, Tehran, Iran).

Synthesis of graphene oxide

1 g graphite powder and sodium nitrate (0.5 g) were added into 25 ml of acid sulfuric and stirred for 10 minutes. Under magnetic stirring, potassium carbonate (3 g) was slowly added into the mixture. Then, the mixture was heated to 35 ^oC and stirred for further 30 min. After that, 45 ml deionized water was added to the mixture and temperature was then raised up to 95 ^oC and stirred for 15 min. Next, add 150 ml deionized water and 10 ml hydrogen peroxide 30% to the solution. The resulting solid phase was filtered and repeatedly washed with hydrochloric acid and deionized water for several times. The obtained solid was graphite oxide and dried at temperature 60^oC for 12 h. The resulting solid was dispersed in deionized water by ultrasonication for making graphene oxide. At the end, the final solid was recovered by centrifugation and dried for 24 h in 60 ^oC. The final brown solid is graphene oxide.

Synthesis of spherical SiO_2 nanoparticles

The mixture of distilled water (20 ml) and ethanol (50 ml) were sonicated for 30 min. Then, 3 ml TEOS was added dropwise within 5 min followed by addition of 0.1 mmol pvp into the mixture under stirring. Thereafter, 0.1 ml ethylenediamine was added dropwise into the mixture as precipitating agent, under ultrasonic. After 30 min, the produced SiO_2 product isolated by centrifugation and washed with ethanol and water three times. The final product was dried at 80 ^oC for overnight.

Synthesis of SiO_2@ CPTES

(0.5 ml, 5 mmol) 3-chloropropyl triethoxysilane (CPTES) was added dropwise to a stirred solution of SiO_2 (1 g) in dry toluene (30 ml) and refluxed for 24 h. After completion of the reaction, the impure product was

separated and washed three times with toluene and dried under 120 °C in a vacuum oven for 8 h to obtain the white powder as SiO_2@CPTES.

Synthesis of SiO_2@ Ethylenediamine (f-SiO_2)

In a 50 ml round-bottomed flask, Ethylenediamine (0.3 g, 1 mmol) was added to the suspension of SiO_2@CPTES (1 g) in absolute ethanol (30 ml) and heated under reflux for 24 h. The resulting solid was collected by filtration and washed successively with ethanol several times and dried at 90 ^oC overnight.

Synthesis of f-SiO_2@GO

0.04 g graphene oxide powder was dispersed in 20 ml deionized water by sonication, then SiO_2@Ethylenediamine (f-SiO_2) (0.16 g) was added to the mixture and sonicated for 20 min. The solution was stirred at 85^oC in an oil bath for 12 h. Lastly, the resulting product was collected by centrifugation, washed with deionized water and ethanol three times, and then dried at 60 ^oC.

Synthesis of f-SiO_2@GO@Co

As-prepared f-SiO_2@GO (0.1 g) with 0.01%wt $CoCl_2$ were dispersed into an absolute ethanol under ultrasound irradiation for 5 min, and then reacted for 24 h at room temperature. The final catalyst was collected and washed with ethanol and deionized water. The product was dried at room temperature for several hours to obtain f-SiO_2@GO@Co catalyst.

General procedure for the synthesis of cis-3-aryl-3a,8b-dihydro-3a,8b-dihydroxy-1 phenylindeno[1,2-c]pyrazol-4(1H)-ones

A mixture of aldehyde (1 mmol) and phenylhydrazine (1 mmol) and 15 mol% f-SiO_2@GO@Co as a catalyst in ethanol (5 ml) were stirred at 60^oC until an intermediate was formed. Next, ninhydrin (1 mmol) was added to the mixture reaction and allowed to stir until the completion of reaction (monitoring by TLC). After that, the heterogeneous catalyst was separated and the crude product was collected and washed with n-hexane and ethyl acetate to achieve the pure final product.

Results And Discussion

Characterization of catalyst

FT-IR spectra for the catalyst preparation steps are reported in Fig. 1. For FT-IR spectrum of GO, the peak at 3398 cm^{-1} is attributed to the O-H group stretching vibrations. The band at 1730 cm^{-1} describes carbonyl stretch for carboxylic acid. The peaks at 1383 and 1060 cm^{-1} assigned to the C–O stretching vibrations and epoxy groups, respectively. The FT-IR spectrum of SiO_2 exhibits the adsorption peaks at 798, 1089 cm^{-1} corresponding to asymmetric vibrations of the Si–O–Si bonds. The band at 3370 cm^{-1}

describes hydroxyl group vibrations. In SiO_2@Cl and SiO_2@Ethylenediamine spectra, the bands at around 950 cm^{-1} is related to ethoxy moieties vibrations. Functionalized graphene oxide shows the characteristic peak in 1102 cm^{-1} which reveals that functionalized SiO_2 was successfully grafted on the graphene oxide.

XRD patterns of the catalyst in different steps are depicted in Fig. 2. GO sheets show a characteristic peak around 12^o which proves the synthesis of graphene oxide. In comparison graphene oxide and functionalized graphene oxide, the new broad peak at $2\theta = 25^o$ is related to amorphous SiO_2 which shows surface functionalization of graphene oxide. The small peak at $2\theta = 44^o$ correspond to cobalt in XRD pattern of final catalyst confirm successful modification of the GO surface.

The SEM images of GO(a) and GO@f-SiO_2@Co (b) has been represented in Fig. 3. The SEM image of graphene oxide clearly shows the layer sheet structure of graphene oxide and GO@f-SiO_2@Co exhibits the surface modification of graphene oxide with functionalized silica nanoparticles.

The presence of Si, Co, C, N in EDS spectrum of the catalyst (Fig. 4) confirm decoration of graphene oxide surface with functionalized SiO_2.

The Raman spectra for GO and GO@f-SiO_2 are shown in Fig. 5. The characteristic peaks for Go at 1362 and 1595 cm^{-1} are attributed to D and G bands, respectively. Also, the spectrum of GO@f-SiO_2 also shows these peaks which confirm the presence of graphene oxide in the structure. In addition, after functionalization of GO slight increase in the ratio of I_D/I_G, indicating more transition from sp^2 to sp^3 from grafting of f-SiO_2 on the graphene oxide.

According to the differential thermal analysis (DTA)/Thermogravimetric analysis (TGA) for the final catalyst (Fig. 6), the primary stage of decomposition occurred at 220 ^oC and continued to 800 ^oC with 18% weight loss in endothermic condition according to the curve of DTA. which is attributed to decomposition of the organic functional groups on the graphene oxide surface.

Catalyst reusability

The important point for a proper catalyst is recovery and recycling. The reusability of f-SiO_2@GO@Co was investigated in the model reaction between phenylhydrazine, ninhydrin, and 2-nitrobenzaldhyde. For checking the reusability, after the completion of the reaction, the catalyst was recovered using filtration, and washed with ethanol to remove impurities and then dried. The recovery of the catalyst was excellent with an average yield (96%) after five times subsequent use. As shown in Fig. 7 the catalyst activity without considerable loss was approximately same for five cycles.

Proposed mechanism

In the first step, reaction of phenylhydrazine (1) with benzaldehyde (2) using f-SiO_2@GO@Co as catalyst to form 1-benzylidene-2-phenylhydrazone (5) intermediate. Next, the intermediate (5) attacks to ninhydrin that was activated by the catalyst to generate zwitterionic (6). Further, its tautomer (7) by intermolecular H-atom transfer an nucleophile addition to a carbonyl group forms indeno[1,2-c]pyrazol- 4(1H)-one derivatives (4a-k) (Scheme 2).

Analysis and characterization of synthesized compound

In order to optimize the reaction conditions, different parameters such as temperature, solvent and catalyst loading were assessed on the model reaction between phenylhydrazine, ninhydrin, and 2-nitrobenzaldehyde. Firstly, the reaction was conducted in MeCN without catalyst in r.t. and, no product was formed after 24 h. When the reaction was carried out in the presence of f-SiO_2@GO@Co in MeCN at 60^oC, no significant yield was formed after 24 h (50%). Also, the reaction was carried out in the presence of f-SiO_2@GO in ethanol and the product was obtained in 75% after 24 h (Table 1, entry4). Then it was tested in ethanol in different temperatures in the presence of f-SiO2@GO@Co as a catalyst (Table 1). The results revealed the yield of product increase at 60 ^oC (Table 1, entry7). According to results shown in Table 1, the best performance of the catalyst was in the presence of ethanol as a solvent. Furthermore, we investigated the effect of catalyst loading (Table 2) and the yield improvement was found with increasing the catalyst from 3 to 15 wt%. It should be mentioned, increasing the more amount of catalyst did not affect on the yield. The performance of the 15 wt% f-SiO_2@GO@Co in the reaction rate in the presence of ethanol as efficient solvent and various aldehydes are given in Table 3.

To confirm the accuracy of desired products (4a–k), we used FT-IR, ^{1}H NMR, and ^{13}CNMR. The IR spectrum of the compound 4i exhibits the peak at 3461 cm^{-1} that is attributed to the stretching vibrations of hydroxyl groups. The strong peak at around 1710 cm^{-1} indicates the presence of carbonyl group. It shows singlet peaks at δ = 7.93 ppm and δ = 7.31 ppm due to hydroxyl groups. The protons on the aromatic rings appear between δ = 8.37 to 7 ppm. In addition, the peak for carbonyl group in ^{13}CNMR appears at 196 ppm. The (C-O) carbons observe in 96.06 and 89.12 ppm.

Table 1

Investigation different temperature and solvents on the reaction [a]

Entry	Solvent	Catalyst	Temperature(°C)	Time	Yield [b] (%)
1	MeCN	-	r.t.	24 h	-
2	MeCN	f-SiO_2@GO@Co	60	24 h	50
3	Ethanol	-	60	24 h	20
4	Ethanol	f-SiO2@GO	60	24 h	75
5	Ethanol	f-SiO_2@GO@Co	25	45	60
6	Ethanol	f-SiO_2@GO@Co	40	30	85
7	Ethanol	f-SiO_2@GO@Co	60	20	96
8	Ethanol/H_2O	f-SiO_2@GO@Co	60	50	89
9	$CHCl_3$	f-SiO_2@GO@Co	60	50	40
a Reaction conditions: phenylhydrazine (1 mmol), 2-nitro benzaldehyde (1 mmol), and ninhydrin (1 mmol) in the presence of f-SiO2@GO@Co as catalyst.					
[b]Isolated yield					

Table 2

Investigation of the amounts of f-SiO_2@GO@Co on the reaction [a]

Entry	Catalyst	Time(min)	Yield[b] (%)
1	3	140	58
2	5	140	75
3	10	50	85
4	15	20	96
[a] Reaction conditions: ethanol (5 ml), phenylhydrazine (1 mmol), 2-nitro benzaldehyde (1 mmol), and ninhydrin (1 mmol) in the presence of SiO_2@GO@Co as catalyst. [b] Isolated yield.			

Spectral Data

Cis-3a,8b-Dihydro-3a,8b-dihydroxy-3-(4-Nitrophenyl)-1-phenyl-indeno[1,2-c]pyrazol-4(1H)-one(4a): Yellow solid; m.p. 235–237 °C; IR (KBr): ν = 3410, 1725, 1594,1528, 1493 cm^{-1}; ^1H NMR (400 MHz, DMSO-d6): δ

= 8.34–8.30 (d, J = 8.8 Hz, 2H), 8.28–8.24(d, J = 8.8 Hz, 2H), 8.07 (s, OH), 7.82–7.78 (d, J = 8.1 Hz, 2H), 7.76–7.72 (m, 2H), 7.68 (d, J = 8.0 Hz, 1H), 7.58 (t, J = 7.6 Hz, 1H), 7.43–7.38 (t, J = 8.0 Hz, 2H), 7.29 (s, OH), 7.09 (t, J = 7.6 Hz, 1H).

Cis-3a,8b-Dihydro-3a,8b-dihydroxy-3-(4-Chlorophenyl)-1-phenyl-indeno[1,2-c]pyrazol-4(1H)-one (4b): Yellow solid, m.p. 229–232 ^{o}C; IR (KBr): = 3273, 1701, 1595, 1489 cm^{-1}; ^{1}H NMR (400 MHz, DMSO-d6): δ = 8.10–8.07 (d, J = 8.3 Hz, 2H), 7.84 (s, OH), 7.76–7.69 (m, 4H), 7.65 (d, J = 8 Hz, 1H), 7.54 (t, J = 7.2 Hz, 1H), 7.48–7.44 (d, J = 8.3 Hz, 2H), 7.39–7.34 (t, J = 8 Hz, 2H), 7.14 (s, OH), 7.03(t, J = 7.5 Hz, 1H).

Cis-3a,8b-Dihydro-3a,8b-dihydroxy-3-(4-Bromophenyl)-1-phenyl-indeno[1,2-c]pyrazol-4(1H)-one (4c): Yellow solid; m.p. 222–225 ^{o}C; IR (KBr): = 3307, 3073, 1701, 1595, 1489 cm^{-1}; ^{1}H NMR (400 MHz, DMSO-d6): δ = 8.10–8.07 (d, J = 8.3 Hz, 2H), 7.97 (s, OH), 7.76–7.69 (m, 4H), 7.67–7.64 (d, J = 8 Hz, 1H), 7.55 (t, J = 7.2 Hz, 1H), 7.48–7.44 (d, J = 8.3 Hz, 2H), 7.33–7.25 (t, J = 8 Hz, 2H), 7.14 (s, OH), 7.02 (t, J = 7.5 Hz, 1H).

Cis-3a,8b-Dihydro-3a,8b-dihydroxy-3-(3-Nitrophenyl)-1-phenyl-indeno[1,2-c]pyrazol-4(1H)-one(4d): Yellow solid; m.p. 242–244 ^{o}C ; IR (KBr): = 3474, 1725, 1596, 1494 cm^{-1}; ^{1}H NMR (400 MHz, DMSO-d6): δ = 8.94 (s, 1H), 8.47 (d, J = 8.0 Hz, 1H), 8.17 (d, J = 8 Hz, 1H), 8.01 (s, OH), 7.81–7.72 (m, 4H), 7.69–7.65 (t, J = 6.1 Hz, 2H), 7.58 (t, J = 7.4 Hz, 1H), 7.42–7.36 (t, J = 7.8 Hz, 2H), 7.29 (s, OH), 7.08 (t, J = 7.4 Hz, 1H).

Cis-3a,8b-Dihydro-3a,8b-dihydroxy-3-(4-methylphenyl)-1-phenyl-indeno[1,2-c]pyrazol-4(1H)-one(4e): Yellow solid; m.p. 253–255 ^{o}C; IR (KBr): = 3439, 3267, 1707, 1595, 1491 cm^{-1}; ^{1}H NMR (400 MHz, DMSO-d6): δ = 7.99–7.96 (d, J = 7.9 Hz, 2H), 7.75–7.67 (m, 5H), 7.63(d, J = 7.9 Hz, 1H), 7.54 (t, J = 7.5 Hz, 1H), 7.39–7.33 (t, J = 7.2 Hz, 2H), 7.22–7.16 (d, J = 7.5 Hz, 2H), 7.03 (s, OH), 6.99 (d, J = 6.7 Hz, 1H), 2.31 (s, 3H).

Cis-3a,8b-Dihydro-3a,8b-dihydroxy-3-(4-methoxyphenyl)-1-phenyl-indeno[1,2-c]pyrazol-4(1H)-one (4f): Orange solid; m.p. 210–213 ^{o}C ;IR (KBr): = 3426, 1708, 1596, 1492 cm^{-1};^{1}H NMR (400 MHz, DMSO): δ = 8.05–8.01 (d, J = 8.4 Hz, 2H), 7.73–7.68 (m, 5H), 7.63 (m, 1H), 7.54 (t, J = 6.2 Hz, 1H), 7.37–7.32 (t, J = 7.1 Hz, 2H), 7.04–6.94 (m, 4H), 3.78 (s, 3H).

Cis-3a,8b-Dihydro-3a,8b-dihydroxy-3-(2-hydroxyphenyl)-1-phenyl-indeno[1,2-c]pyrazol-4(1H)-one(4 g): Yellow solid; m.p. 190–193 ^{o}C; IR (KBr): =3392, 1724, 1595, 1491 cm^{-1}; ^{1}H NMR (400 MHz, DMSO): δ = 10.4 (s, OH), 8.29 (d, J = 8 Hz, CH), 7.90 (s, OH), 7.75-–7.69 (m, 2CH), 7.58– 7.55 (m, 3CH), 7.51 (d, J = 7.9 Hz, 1H), 7.44–7.39 (t, J = 8 Hz, 2CH), 7.34 (s, OH), 7.24 (t, J = 8 Hz, 1H), 7.11 (t, J = 7.2 Hz, 1H), 6.96 (t, J = 7.2 Hz, 1H), 6.89 (d, J = 8.1 Hz, 1H).

cis-3a,8b-Dihydro-3a,8b-dihydroxy-1,3-diphenylindeno[1,2-c]pyrazol-4(1H)-one(4 h): Yellow solid; m.p. 219–222 ^{o}C; IR (KBr): =3430, 1706, 1594,1491 cm^{-1}; ^{1}H NMR (400 MHz, DMSO-d6): δ = 8.12–8.07 (d, J = 8 Hz, 2H), 7.77–7.72 (d, J = 8.0 Hz, 2H), 7.69–7.62 (m, 3H), 7.52–7.48 (t, J = 7.2 Hz, 2H), 7.38–7.26 (m, 6H), 6.97(t, J = 7.2 Hz, 1H).

Cis-3a,8b-Dihydro-3a,8b-dihydroxy-3-(2-Nitrophenyl)-1-phenyl-indeno[1,2-c]pyrazol-4(1H)-one(4i): Yellow solid; m.p. 165–168 ^{o}C; IR (KBr): =3461, 1710, 1597, 1530 cm^{-1}; ^{1}H NMR (400 MHz, DMSO-d6)= δ = 8.38 (d, J = 8 Hz, 1H), 7.93(s, OH), 7.78–7.69 (m, 4H), 7.61–7.50 (m, 5H), 7.40–7.34 (t, J = 8 Hz, 2H), 7.31 (s, OH), 7.06 (t, J = 7.2 Hz, 1H); ^{13}C NMR (DMSO): δ = 196.63 (C = O), 148.54 (C), 147.60 (C), 141.732 (C), 137.56 (C), 137.24 (C), 136.78 (C), 134.34 (CH), 130.99 (CH), 130.76 (CH), 129.93 (CH), 129.04 (2CH), 125.35 (CH), 123.88 (CH), 123.28 (CH), 123.24 (CH), 122.74 (CH), 117.49 (2CH), 96.06 (C), 89.12 (C).

Cis-3a,8b-Dihydro-3a,8b-dihydroxy-3-(2,3-dihydroxyphenyl)-1-phenyl-indeno[1,2-c]pyrazol-4(1H)-one (4j): Yellow solid; m.p. 222–224 ^{o}C; IR (KBr): 3473, 3365,1726, 1598, 1494 cm^{-1}; ^{1}H NMR (400 MHz, DMSO): δ = 10.45 (s, OH), 8.91 (s, OH), 7.89 (s, OH), 7.78– 7.66 (m, 3H), 7.6– 7.54 (m, 3H), 7.50 (d, J = 6.9 Hz, 1H), 7.45–7.39 (dd, J = 6.8, 2H), 7.32 (s, 1H), 7.18–7.07 (m, 1H), 6.81–6.71 (m, 2H). ^{13}C NMR (DMSO-d6): δ = 197.00 (C), 156.40 (C), 147.51 (C), 145.34 (C), 141.28 (C), 136.84 (C), 134.19 (C), 130.77 (C), 129.98 (CH), 129.34 (2CH), 129.25 (CH), 125.39 (CH), 123.42 (CH), 122.91 (CH), 118.89 (CH), 117.73 (2CH), 116.06 (CH), 115.08(CH), 94.71 (C), 89.66 (C).

Cis-3a,8b-Dihydro-3a,8b-dihydroxy-3-(2-hydroxy-5-Bromo-phenyl)-1-phenyl-indeno[1,2-c]pyrazol-4(1H)-one (4 k): Yellow solid, m.p. 226–228 ^{o}C; IR (KBr): 3324, 3192, 1735, 1597, 1488 cm^{-1}; ^{1}H NMR (400 MHz, DMSO): δ = 10.47 (s, OH), 8.43 (s, 1H), 8.03 (s, 1H), 7.77 (d, J = 7.6 Hz, 1H), 7.72 (d, J = 7.6 Hz, 1H), 7.62–7.56 (t, J = 6.9 Hz, 3H), 7.53 (d, J = 8 Hz, 1H), 7.45–7.36 (m, 4H), 7.12 (t, J = 7.2 Hz, 1H), 6.87 (d, J = 8.3 Hz, 1H).

^{13}C NMR (DMSO-d_6): δ = 196.83 (C = O), 155.50 (C), 147.53 (C), 143.57 (C), 141.00(C), 137.00 (C),134.13(C), 132.19 (C), 131.14 (CH), 130.85 (CH), 129.28 (2CH), 125.40 (CH), 123.58 (CH), 123.22 (CH), 118.33 (CH), 117.93 (2CH), 117.10 (CH), 110.15 (CH), 94.80 (C), 89.27 (C).

Conclusion

In summary, we have synthesized GO@f-SiO_2@Co as a heterogenous and recoverable catalyst which was an efficient catalyst for synthesis of indenopyrazolones derivatives. Results showed the catalyst with high catalytic activity provided excellent yields in a shorter reaction time under mild conditions.

Declarations

Ethics approval and consent to participate

Not applicable

Consent for publication

The authors declare that the copyright belongs to the journal

Availability of data and materials

All data are fully available without restriction

Competing interests

None of the authors have any competing interests in the manuscript

Funding

Not applicable

Authores contributions

MM designed, carried out the literature study, performed the assay, conducted the optimization, purification of compounds and prepared the manuscript. Furthermore, performed the related analyses. All authors read and approved the final manuscript. JSG have designed the study, participated in discussing results and revised the manuscript.

Authores information

Department of Organic Chemistry, Faculty of Chemistry, University of Kashan, Kashan, P.O. Box 87317-51167, I. R. Iran.

Acknowledgment

We are very grateful for Kashan university from the financial support to run this project.

Associated content

Experimental procedure and product characterization data: IR, ^{1}H NMR, ^{13}C NMR of the compounds are reported in Additional file 1.

References

1. Chaurasia SR, Dange R, Bhanage BM (2020) Graphene oxide as a carbo-catalyst for the synthesis of tri-substituted 1,3,5-triazines using biguanides and alcohols. Catal Commun 137:105933. https://doi.org/10.1016/j.catcom.2020.105933
2. Novoselov KS, Geim AK, Morozov SV et al (2004) Electric Field Effect in Atomically Thin Carbon Films. Science 306:666–669. https://doi.org/10.1126/science.1102896
3. Ray SC (2015) Application and Uses of Graphene Oxide and Reduced Graphene Oxide. Elsevier Inc
4. Aday B, Pamuk H, Kaya M, Sen F (2016) Graphene oxide as highly effective and readily recyclable catalyst using for the one-pot synthesis of 1,8-dioxoacridine derivatives. J Nanosci Nanotechnol 16:6498–6504. https://doi.org/10.1166/jnn.2016.12432

5. Bozkurt S, Tosun B, Sen B et al (2017) A hydrogen peroxide sensor based on TNM functionalized reduced graphene oxide grafted with highly monodisperse Pd nanoparticles. Anal Chim Acta 989:88–94. https://doi.org/10.1016/j.aca.2017.07.051
6. Hajian R, Fung K, Chou PP et al (2019) Properties and Applications of Functionalized Graphene Oxide. Mater Matters 14:37–45
7. Chen D, Feng H, Li J (2012) Graphene oxide: Preparation, functionalization, and electrochemical applications. Chem Rev 112:6027–6053. https://doi.org/10.1021/cr300115g
8. Lavin-Lopez MDP, Romero A, Garrido J et al (2016) Influence of different improved hummers method modifications on the characteristics of graphite oxide in order to make a more easily scalable method. Ind Eng Chem Res 55:12836–12847. https://doi.org/10.1021/acs.iecr.6b03533
9. Shi X, Nguyen TA, Suo Z et al (2009) Effect of nanoparticles on the anticorrosion and mechanical properties of epoxy coating. Surf Coatings Technol 204:237–245. https://doi.org/10.1016/j.surfcoat.2009.06.048
10. Wang T, Ge H, Zhang K (2018) A novel core-shell silica@graphene straticulate structured antistatic anticorrosion composite coating. J Alloys Compd 745:705–715. https://doi.org/10.1016/j.jallcom.2018.02.222
11. Kaur A, Gangacharyulu D, Bajpai PK (2018) Catalytic hydrogen generation from NABH4/H2O system: Effects of catalyst and promoters. Brazilian J Chem Eng 35:131–139. https://doi.org/10.1590/0104-6632.20180351s20150782
12. Li X, He L, Chen H et al (2013) Copper-catalyzed aerobic C(sp2)-H functionalization for C-N bond formation: Synthesis of pyrazoles and indazoles. J Org Chem 78:3636–3646. https://doi.org/10.1021/jo400162d
13. Kiyani H, Albooyeh F, Fallahnezhad S (2015) Synthesis of new pyrazolyl-1,3-diazabicyclo[3.1.0]hexe-3-ene derivatives. J Mol Struct 1091:163–169. https://doi.org/10.1016/j.molstruc.2015.02.069
14. Özdemir Z, Kandilci HB, Gümüşel B et al (2007) Synthesis and studies on antidepressant and anticonvulsant activities of some 3-(2-furyl)-pyrazoline derivatives. Eur J Med Chem 42:373–379. https://doi.org/10.1016/j.ejmech.2006.09.006
15. Rangaswamy J, Vijay Kumar H, Harini ST, Naik N (2012) Synthesis of benzofuran based 1,3,5-substituted pyrazole derivatives: As a new class of potent antioxidants and antimicrobials-A novel accost to amend biocompatibility. Bioorganic Med Chem Lett 22:4773–4777. https://doi.org/10.1016/j.bmcl.2012.05.061
16. Lv PC, Li HQ, Sun J et al (2010) Synthesis and biological evaluation of pyrazole derivatives containing thiourea skeleton as anticancer agents. Bioorganic Med Chem 18:4606–4614. https://doi.org/10.1016/j.bmc.2010.05.034
17. Vicentini CB, Romagnoli C, Andreotti E, Mares D (2007) Synthetic pyrazole derivatives as growth inhibitors of some phytopathogenic fungi. J Agric Food Chem 55:10331–10338. https://doi.org/10.1021/jf072077d

18. Singer RA, Doré M, Sieser JE, Berliner MA (2006) Development of nonproprietary phosphine ligands for the Pd-catalyzed amination reaction. Tetrahedron Lett 47:3727–3731. https://doi.org/10.1016/j.tetlet.2006.03.132
19. Porzelle A, Woodrow MD, Tomkinson NCO (2009) Palladium-catalyzed coupling of hydroxylamines with aryl bromides, chlorides, and iodides. Org Lett 11:233–236. https://doi.org/10.1021/ol8025022
20. Hosseini Nasab N, Safari J (2019) The Novel Synthesis of Functionalized Indenopyrazolones Using Fe 3 O 4 nanoparticles stabilized on MMT: An Efficient Magnetically Recoverable Heterogeneous Nanocomposite Catalyst. J Heterocycl Chem 56:915–921. https://doi.org/10.1002/jhet.3469
21. Yavari I, Seyfi S, Skoulika S (2012) A convenient synthesis of functionalized indenopyrazolones from indan-1,2,3-trione, benzaldehydes, and phenylhydrazine. Helv Chim Acta 95:1581–1585. https://doi.org/10.1002/hlca.201200053

Tables

Due to technical limitations, table 3 is only available as a download in the Supplemental Files section.

Figures

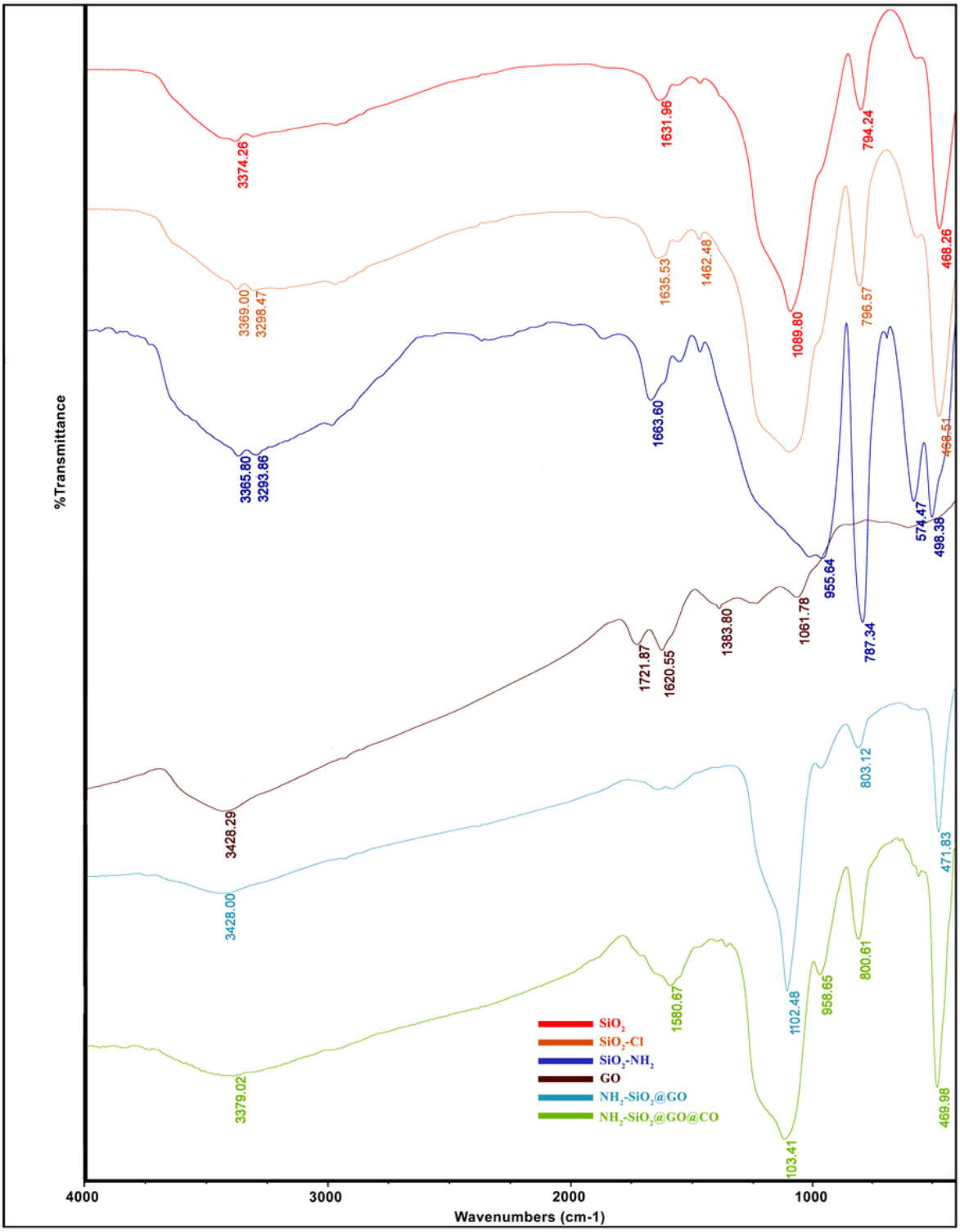

Figure 1

FT-IR spectra of SiO2, SiO2@Cl, SiO2@NH2, GO, f-SiO2@GO, and f-SiO2@GO@Co

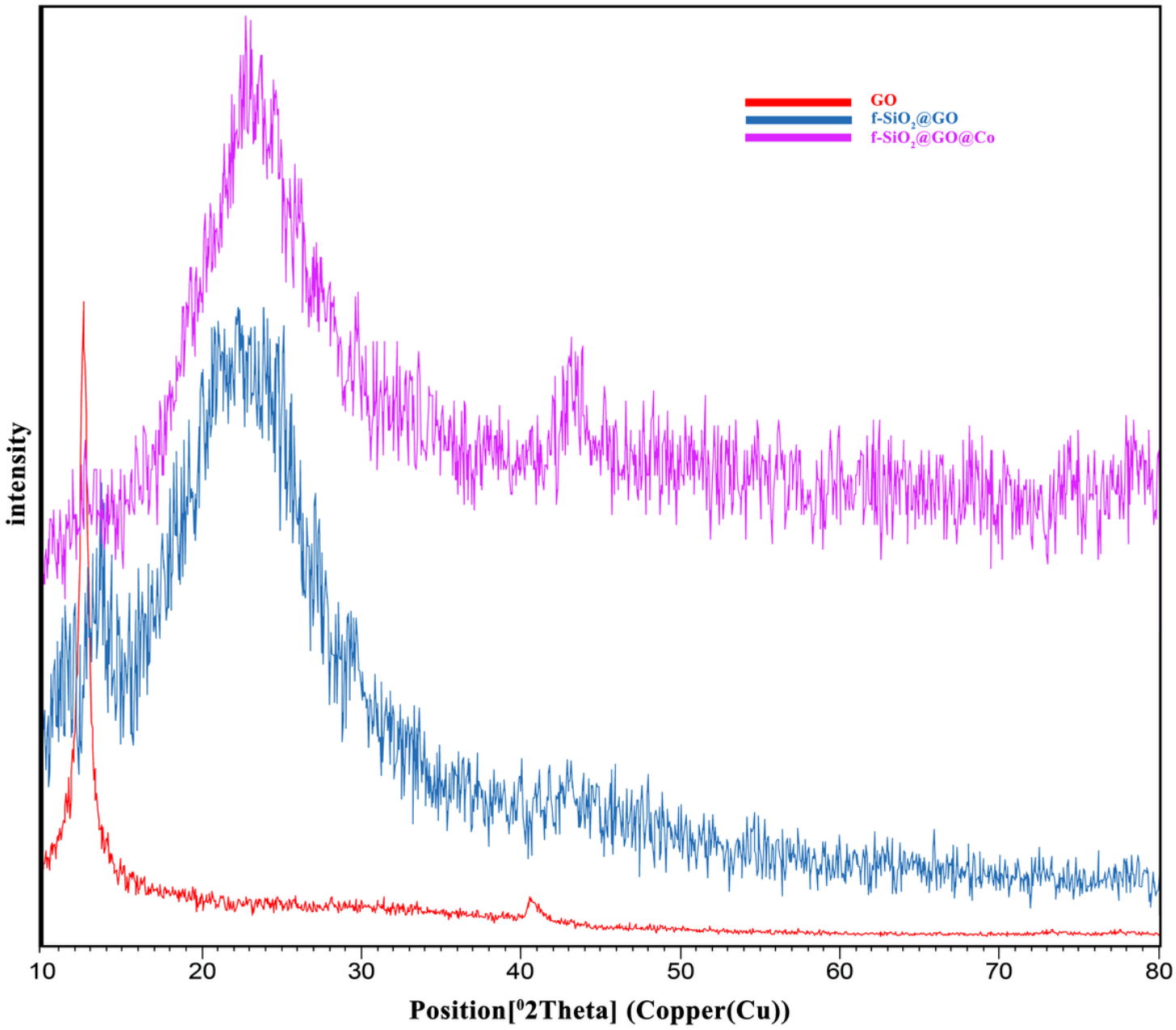

Figure 2

XRD patterns of GO, f-SiO2@GO, and f-SiO2@GO@Co

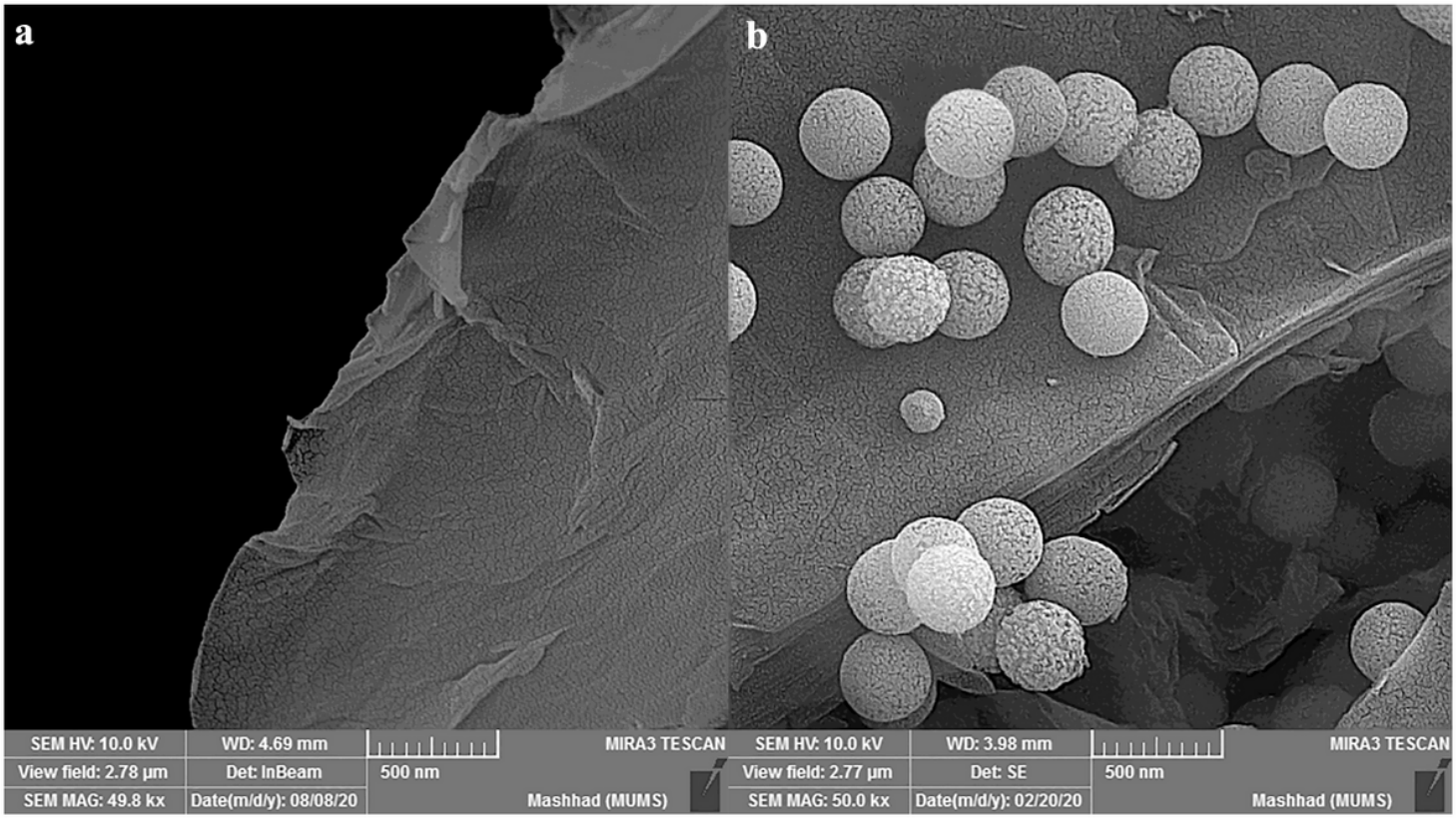

Figure 3

FE-SEM images of GO, f-SiO2@GO@Co

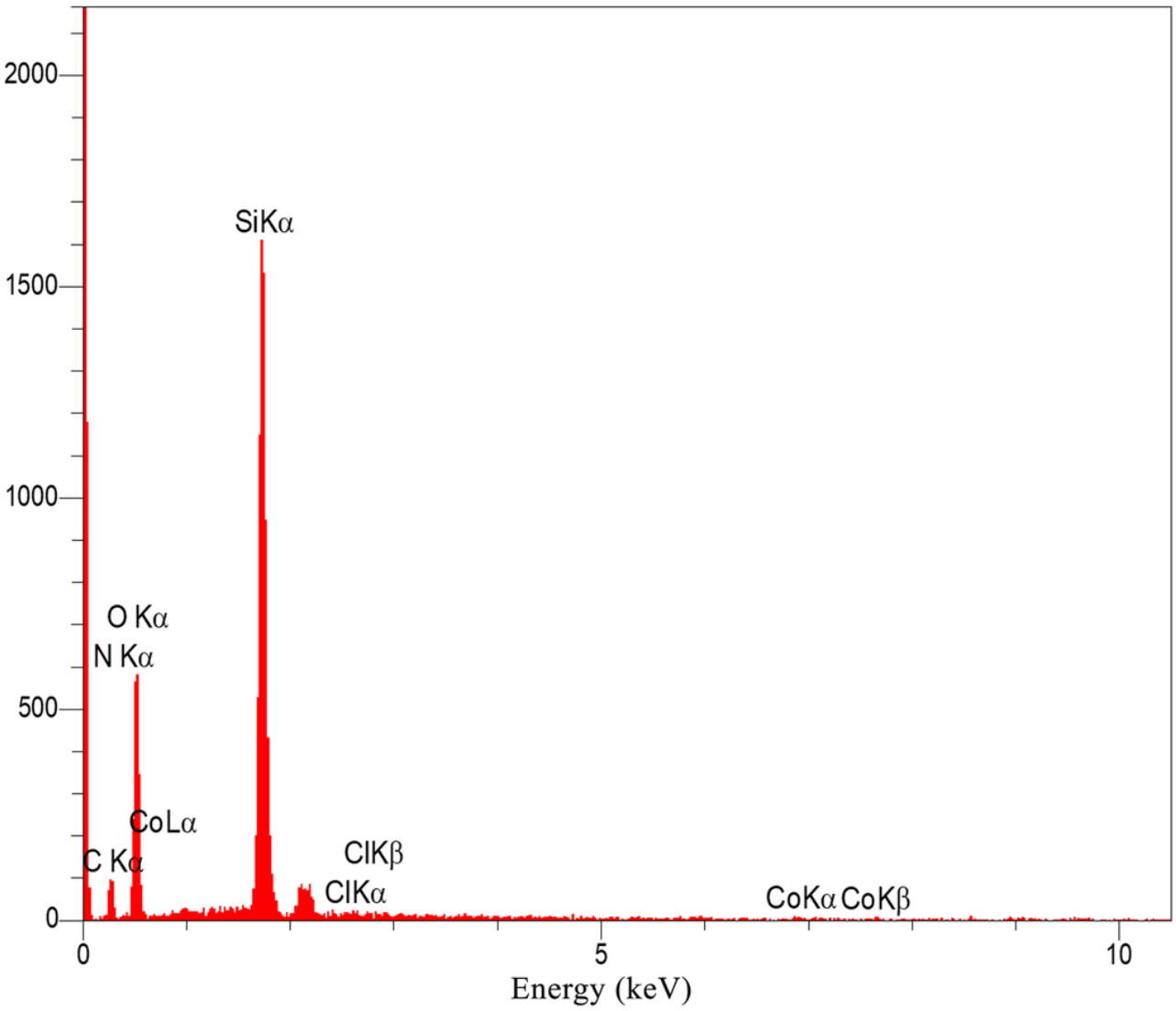

Figure 4

EDS spectrum of f-SiO2@GO@Co

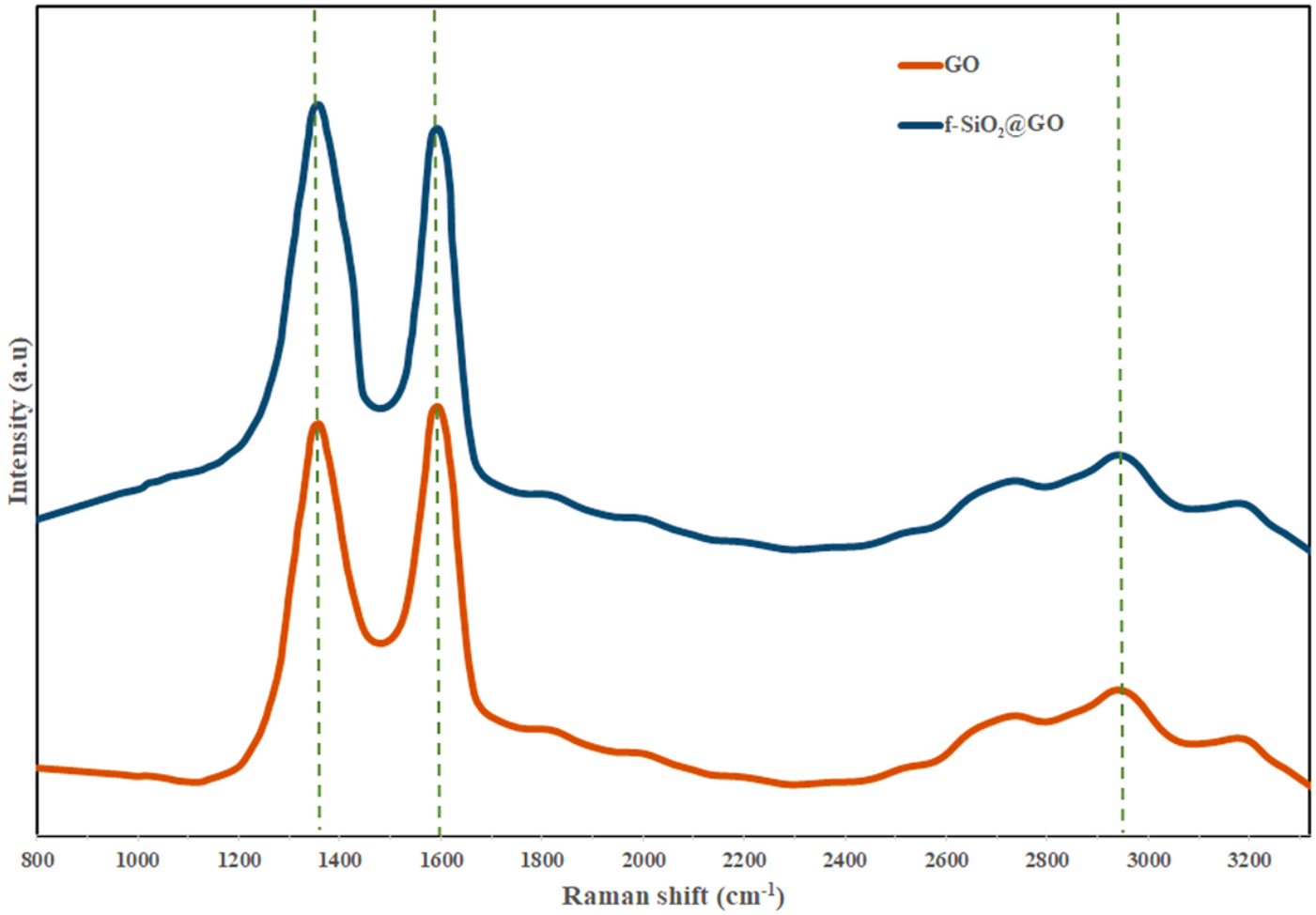

Figure 5

Raman spectra of GO and f-SiO2@GO

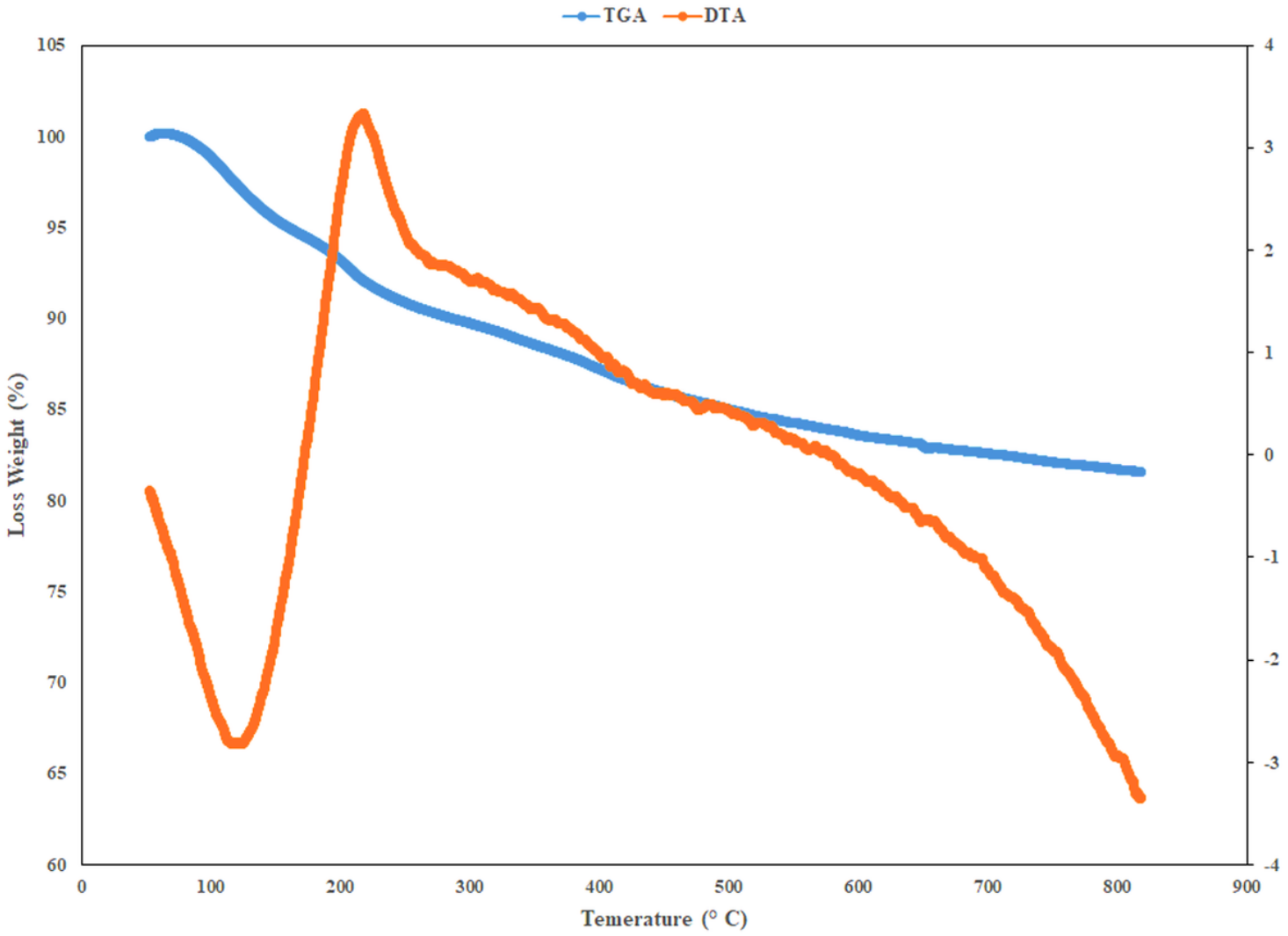

Figure 6

TGA and DTA curve of f-SiO2@GO@Co

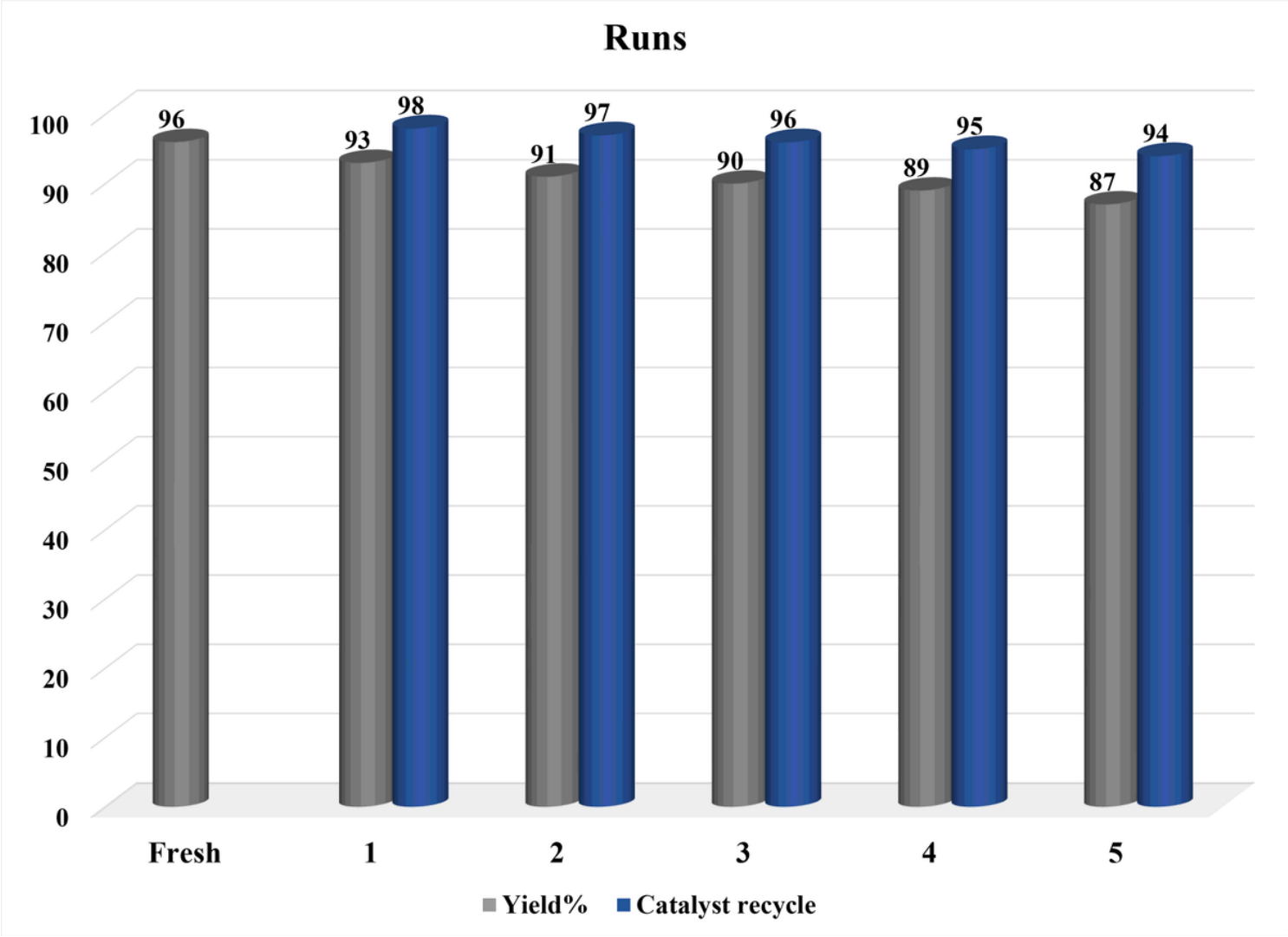

Figure 7

Recycling results of f-SiO2@GO@Co

Supplementary Files

This is a list of supplementary files associated with this preprint. Click to download.

- Table3.JPG
- Table3a.JPG
- Supplymentaryinformation.docx
- OnlineScheme1.Png
- OnlineScheme2.Png
- GraphicalAbstract.jpg